

# Gravitational wave radiation from the coalescence of white dwarfs

P. Lorén-Aguilar<sup>1,2</sup>, J. Guerrero<sup>1,2</sup>, J. Isern<sup>1,2</sup>, J.A. Lobo<sup>1,3</sup> and E. García-Berro<sup>1,4</sup>

<sup>1</sup>*Institut d'Estudis Espacials de Catalunya, Edifici Nexus, Gran Capità 2-4, 08034 Barcelona, Spain*

<sup>2</sup>*Institut de Ciències de l'Espai, C.S.I.C*

<sup>3</sup>*Departament de Física Fonamental, Universitat de Barcelona, c/Martí i Franquès 1, 08028 Barcelona, Spain.*

<sup>4</sup>*Departament de Física Aplicada, Universitat Politècnica de Catalunya, Escola Politècnica Superior de Castelldefels, Avda. del Canal Olímpic s/n, 08860 Castelldefels, Spain.*

4 November 2018

## ABSTRACT

We compute the emission of gravitational radiation from the merging of a close white dwarf binary system. This is done for a wide range of masses and compositions of the white dwarfs, ranging from mergers involving two He white dwarfs, mergers in which two CO white dwarfs coalesce to mergers in which a massive ONe white dwarf is involved. In doing so we follow the evolution of binary system using a Smoothed Particle Hydrodynamics code. Even though the coalescence process of the white dwarfs involves considerable masses, moving at relatively high velocities with a high degree of asymmetry we find that the signature of the merger is not very strong. In fact, the most prominent feature of the coalescence is that in a relatively small time scale (of the order of the period of the last stable orbit, typically a few minutes) the sources stop emitting gravitational waves. We also discuss the possible implications of our calculations for the detection of the coalescence within the framework of future space-borne interferometers like LISA.

**Key words:** stars: white dwarfs — gravitational waves — binaries: close

## 1 INTRODUCTION

Gravitational waves are a direct consequence of the General Theory of Relativity. Many efforts have been done so far to detect them, but due to the intrinsic experimental difficulties involved in the process of detection and in the data analysis no definite result has been yet obtained. Supernova core collapse, binary systems involving compact objects, like double black holes, double neutron stars or double white dwarfs are, amongst others, promising sources of gravitational waves — see Schutz (1999) for a comprehensive review on the subject. Moreover, with the advent of the current generation of terrestrial gravitational wave detectors, like LIGO (Abramovici et al. 1992), VIRGO (Acernese et al. 2004), GEO600 (Willke et al. 2004), or TAMA (Takahashi et al. 2004), and of space-borne interferometers like LISA<sup>1</sup> (Bender et al. 1998, 2000), gravitational wave astronomy will probably be soon a tangible reality.

As already mentioned, one of the most promising sources of gravitational waves are galactic binary systems containing at least one compact object. Galactic binaries, such as neutron stars binaries, cataclysmic binaries or

close white dwarf binaries, are guaranteed sources for LISA (Mironowsky 1965; Evans, Iben & Smarr 1987), provided that the sources are at sufficiently close distances. In fact, emission from galactic close white dwarf binary systems is expected to be the dominant contribution to the background noise in the low frequency region, which ranges from  $\sim 10^{-3}$  up to  $\sim 10^{-2}$  Hz (Bender et al. 1998). Additionally, from very simple considerations about the initial mass function, it is easy to see that galactic close white dwarf binaries must be quite common (Hils, Bender & Webbink 1990) and, consequently, if the amplitude of the gravitational waves is large enough we should be able to eventually detect them during the operation of LISA. Moreover, the merging of two white dwarfs by emission of gravitational radiation will be the final destiny of a good fraction of this type of binary systems. Since during the merging process a sizeable amount of gravitational waves is expected to be produced (Guerrero et al. 2004) it is important to characterize which would be the gravitational wave emission of such process and to assess the feasibility of detecting them.

The process of formation of close white dwarf binaries involves two mass transfer episodes of the progenitor stars when each of the components of the binary system evolves off the main sequence. Depending on when during the lives of the binary components the mass transfer

<sup>1</sup> <http://lisa.jpl.nasa.gov>

episodes occur the components may have different core compositions. In particular, we may have He-He systems with a total mass  $M_{\text{tot}} \lesssim 0.75 M_{\odot}$ , He-CO for those systems with masses within the range  $0.75 M_{\odot} \lesssim M_{\text{tot}} \lesssim 1.45 M_{\odot}$ , CO-CO for masses larger than  $M_{\text{tot}} \sim 1.45 M_{\odot}$  and even He-ONe or CO-ONe systems when one of the white dwarfs is a massive one. Although the astrophysical scenarios in which a merger of two white dwarfs in a close binary system can occur and their relative frequencies have been relatively well studied — see, for instance, Yungelson et al. (1994), and Nelemans et al. (2001a, 2001b), and references therein — the process of merging itself has received little attention until very recently. Indeed, one of the probable reasons for this lack of theoretical models is the heavy computational demand involved in the simulation of an intrinsically three-dimensional phenomenon. However, in sharp contrast, the coalescence of two neutron stars has been extensively studied — see, for instance, Rosswog et al. (2000), Rosswog & Davies (2002), and Rosswog & Liebendörfer (2003), and references therein, for some of the most recent works on this subject.

In a recent paper (Guerrero et al. 2004) we thoroughly studied the merging of white dwarf binary systems for a wide range of masses and compositions. In doing this we used an up-to-date *Smoothed Particle Hydrodynamics* code. This method was first proposed by Lucy (1977) and, independently, by Gingold & Monaghan (1977). The fact that the method is totally Lagrangian and does not require a grid makes it specially suitable for studying an intrinsically three-dimensional problem like the coalescence of two white dwarfs. In the present paper we will not discuss the simulations presented there. The interested reader can find them in mpeg format at the following URL: <ftp://ftp.ieec.fcr.es/pub/astrofisica/SPH>. Instead, in this paper we compute the gravitational wave signature expected from the merging of two white dwarfs as obtained from those SPH calculations. The paper is organized as follows. In §2 we briefly describe the main ingredients of our SPH code, whereas in §3 we summarize the physics of the emission of gravitational waves. In §4 we discuss the calibration and consistency checks we have done in order to assess the reliability of our results, whereas in §5 and §6 we present our results. Finally, in §7 we summarize our results and draw our conclusions.

## 2 THE SMOOTHED PARTICLE HYDRODYNAMICS CODE

We follow the coalescence of the binary system using a Lagrangian particle numerical code and, more specifically, a Smoothed Particle Hydrodynamics (SPH) code. Our SPH code has been described at length in Guerrero et al. (2004). However, for the sake of completeness we provide here a short description of the main input physics and numerical techniques. Our code follows closely the prescriptions of Benz (1990), where the basic numerical scheme for solving the hydrodynamic equations can be found. We use the standard polynomial kernel of Monaghan & Lattanzio (1985). The gravitational forces are evaluated using an oct-tree (Barnes & Hut 1986). The artificial viscosity adopted in this work is that of Balsara (1995). Regarding the integration method we use a predictor-corrector numerical scheme

with variable time step (Serna, Alimi & Chieze 1996), which turns out to be quite accurate. The adopted equation of state is the sum of three components. The ions are treated as an ideal gas but taking into account the coulombian corrections. We have also incorporated the pressure of photons. Finally, the most important contribution is the pressure of degenerate electrons which is treated as the standard zero temperature expression plus the temperature corrections. The nuclear network adopted here (Benz, Hill, & Thielemann 1989) incorporates 14 nuclei: He, C, O, Ne, Mg, Si, S, Ar, Ca, Ti, Cr, Fe, Ni and Zn. The reactions considered are captures of  $\alpha$  particles, and the associated back reactions, the fusion of two C nuclei, and the reaction between C and O nuclei. All the rates are taken from Rauscher & Thielemann (2000). The thermal evolution of the system is followed in two ways. On the one hand the variation of the internal energy is followed according to:

$$\frac{du_i}{dt} = \frac{P_i}{\rho_i^2} \sum_{j=1}^N m_j \vec{v}_{ij} \cdot \vec{\nabla}_i W(r_{ij}, h) \quad (1)$$

where  $W(r_{ij}, h)$  is the smoothing kernel and the rest of the symbols have their usual meaning. The smoothing length adopted in this work is the linear average of the particles considered in the corresponding calculation; that is  $h_{ij} = (h_i + h_j)/2$ . On the other, we simultaneously compute the temperature variation according to:

$$\frac{dT_i}{dt} = - \sum_{j=1}^N \frac{m_j}{(C_v)_j} \frac{T_j}{\rho_j} \left[ \left( \frac{\partial P}{\partial t} \right)_{\rho_j} \right] \vec{v}_{ij} \cdot \vec{\nabla}_i W(r_{ij}, h) \quad (2)$$

If in the region under study the temperature is below  $6 \times 10^8$  K or the density is smaller than  $6 \times 10^3$  g/cm<sup>3</sup> we use equation (2) otherwise we use equation (1). We have found that in this way energy is better conserved.

## 3 EMISSION OF GRAVITATIONAL WAVES

We compute the gravitational wave emission in the slow-motion, weak-field quadrupole approximation (Misner et al. 1973). The dimensionless wave strain,  $h$ , in the transverse-traceless gauge is given by:

$$h_{jk}^{\text{TT}}(t, \mathbf{x}) = \frac{2G}{c^4 d} \frac{\partial^2 Q_{jk}^{\text{TT}}(t - R)}{\partial t^2} \quad (3)$$

where  $t - R = t - d/c$  is the retarded time,  $d$  is the distance to the observer and  $Q_{jk}^{\text{TT}}(t - R)$  is the reduced quadrupole moment of the mass distribution, which is given by:

$$Q_{jk}^{\text{TT}}(t - R) = \int \rho(\mathbf{x}, t - R) (x^j x^k - \frac{1}{3} x^2 \delta_{jk}) d^3 x \quad (4)$$

The rest of the symbols have their usual meaning. It is useful to express the time derivative of the quadrupole moment in the following way (Nakamura & Oohara 1989):

$$\ddot{Q}_{jk}^{\text{TT}}(t - R) = P_{ijkl}(\mathbf{N}) \int d^3 x \rho [2v^k v^l - x^k \partial^l \phi - x^l \partial^k \phi] \quad (5)$$

where

$$\begin{aligned} P_{ijkl}(\mathbf{N}) &\equiv (\delta_{ij} - N_i N_j)(\delta_{kl} - N_k N_l) \\ &- \frac{1}{2}(\delta_{ij} - N_i N_j)(\delta_{kl} - N_k N_l) \end{aligned} \quad (6)$$

is the transverse-traceless projection operator onto the plane orthogonal to the outgoing wave direction,  $\mathbf{N}$ , and  $\phi$  is the gravitational potential. Now, one can express Eq. (3) in the following way:

$$h_{jk}^{\text{TT}}(t, \mathbf{x}) = \frac{G}{c^4 d} (A_+(t, \mathbf{x}) \mathbf{e}_{+jk} + A_\times(t, \mathbf{x}) \mathbf{e}_{\times jk}) \quad (7)$$

where the polarization tensor coordinate matrices are defined as:

$$\mathbf{e}_{+jk} = \frac{1}{\sqrt{2}} [(\mathbf{e}_x)_j (\mathbf{e}_x)_k - (\mathbf{e}_y)_j (\mathbf{e}_y)_k] \quad (8)$$

$$\mathbf{e}_{\times jk} = \frac{1}{\sqrt{2}} [(\mathbf{e}_x)_j (\mathbf{e}_y)_k + (\mathbf{e}_y)_j (\mathbf{e}_x)_k],$$

the dimensionless amplitudes  $h_+ \equiv A_+/d$  and  $h_\times \equiv A_\times/d$  are the two independent modes of polarization in the transverse-traceless gauge, and the amplitudes are respectively given by

$$A_+(t, \mathbf{x}) = \ddot{Q}_{xx} - \ddot{Q}_{yy}, \quad A_\times(t, \mathbf{x}) = +2\ddot{Q}_{xy} \quad (9)$$

for  $i = 0$ , and

$$A_+(t, \mathbf{x}) = \ddot{Q}_{zz} - \ddot{Q}_{yy}, \quad A_\times(t, \mathbf{x}) = -2\ddot{Q}_{yz} \quad (10)$$

for  $i = \pi/2$ .

In our case we have a collection of  $n$  individual SPH particles. Consequently, Eq. (5) must be discretized and it is computed according to the following expression:

$$\begin{aligned} \ddot{Q}_{jk}^{\text{TT}}(t - R) &\approx P_{ijkl}(\mathbf{N}) \sum_{p=1}^n m(p) [2\mathbf{v}^k(p) \mathbf{v}^l(p) \\ &+ \mathbf{x}^k(p) \mathbf{a}^l(p) + \mathbf{x}^l(p) \mathbf{a}^k(p)] \end{aligned} \quad (11)$$

Where  $m(p)$  is the mass of each SPH particle, and  $\mathbf{x}(p)$ ,  $\mathbf{v}(p)$  and  $\mathbf{a}(p)$  are, respectively, its position, velocity and acceleration.

#### 4 CALIBRATION AND CONSISTENCY CHECKS

We have done two tests, gravitational wave emission from a single, isolated star, and gravitational wave emission from a close white dwarf binary system in a circular orbit. For both cases there exist analytical solutions to which we can compare our numerical results. In the first case, we have followed the time evolution of an isolated  $1 M_\odot$  star using  $2 \times 10^4$  SPH particles of the same mass. For the second test we have followed the evolution of a binary system made of two white dwarfs of the same mass ( $1 M_\odot$ ) in a circular orbit. Each one of the white dwarfs was simulated using  $2 \times 10^4$  SPH particles of the same mass.

The first of our tests was designed to set the zero point of our calculations. Since in SPH simulations the particles are allowed to move freely under the action of their own gravitational potential and of the pressure forces, and since the mass of each particle is relatively large it is not obvious *a priori* whether or not a stable relaxed configuration radiates gravitational waves. Figure 1 shows the dimensionless strains for the case of an isolated white dwarf. We only show times larger than 60 s, for which the star is already

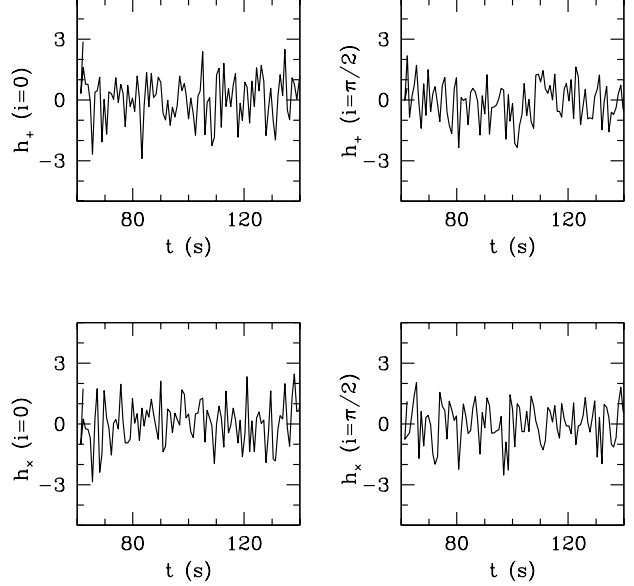


**Figure 1.** Gravitational wave emission from an isolated, spherical star. The dimensionless strains  $h_+$  and  $h_\times$  are measured in units of  $10^{-25}$ . The source is located at a distance of 10 kpc.

relaxed to its final configuration. The relaxation procedure consisted in allowing the initial configuration (which consisted in randomly distributing the SPH particles according to the density profile of a zero temperature white dwarf of the same mass) to evolve for a long enough time until the oscillations of the resulting configuration were completely negligible. In this way we check whether or not the numerical noise produces a negligible emission of gravitational waves. And this is indeed the case. As it can be seen the emission of gravitational waves is negligible, as it should be, given that the relaxed configuration presents spherical symmetry — see Eq. (4).

With regard to the second test, it is worth recalling that the emission of gravitational waves from a binary system, can be obtained quite easily by assuming that both stars are point-like mass distributions. By doing so, from Eqs. (3) and (4) one obtains

$$h_+ = \sqrt{2} \frac{\mu}{d} \frac{G^{\frac{5}{3}}}{c^4} (\omega M_{\text{tot}})^{\frac{2}{3}} (1 + \cos^2 i) \cos 2\omega t \quad (12)$$

and

$$h_\times = 2\sqrt{2} \frac{\mu}{d} \frac{G^{\frac{5}{3}}}{c^4} (\omega M_{\text{tot}})^{\frac{2}{3}} (\cos i) \sin 2\omega t, \quad (13)$$

where  $\omega$  is the angular velocity of the stars,  $\mu$  is the reduced mass,  $M$  is the mass of the white dwarfs, and  $i$  is the observation angle with respect to the orbital plane.

In our SPH simulations we have chosen the binary system to have a separation of  $0.05 R_\odot$  or, equivalently,  $\omega = 7.94 \times 10^{-2} \text{ s}^{-1}$ . The two white dwarfs describe circular orbits and no mass is transferred between both components. Moreover, the two white dwarfs preserve their initial spherical symmetry. Hence, and according to Eqs. (12) and (13), we should expect to obtain dimensionless strains which are

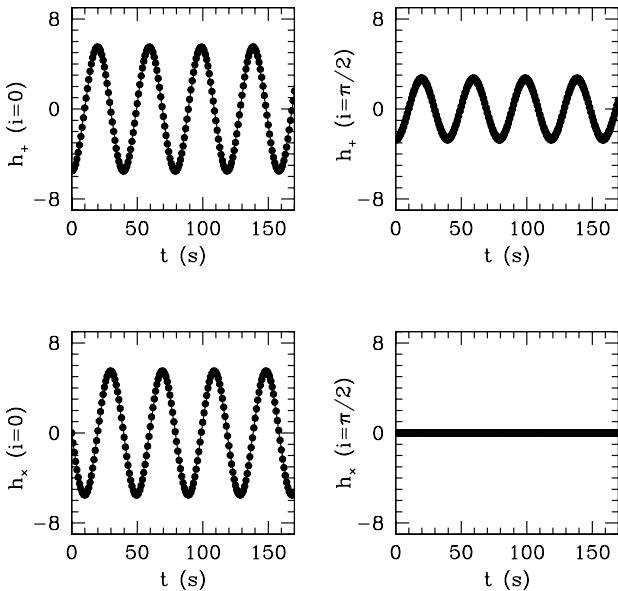


**Figure 2.** Gravitational wave emission from a close white dwarf binary system. The dimensionless strains  $h_+$  and  $h_x$  are measured in units of  $10^{-22}$ . The solid line corresponds to the theoretical solution whereas the dots correspond to our numerical solution. Again, the source is assumed to be at a distance of 10 kpc.

**Table 1.** Summary of the simulations discussed in this paper. The number of SPH particles for the simulations of the first section of the table is  $4 \times 10^4$ , whereas for the last simulation is  $4 \times 10^5$ .

Run	$M_{\text{tot}} (M_{\odot})$	Composition	$R_0 (R_{\odot})$	$t$ (s)
1	0.4+1.2	He/ONe	0.040	180
2	0.4+0.4	He/He	0.042	600
3	0.6+0.6	CO/CO	0.041	180
4	0.6+1.0	CO/CO	0.038	725
5	0.6+0.8	CO/CO	0.033	600
6	0.8+1.0	CO/CO	0.028	1000
7	0.6+0.6	CO/CO	0.040	90

sinusoidal functions with a period equal to half of the orbital period. As it can be seen from Figure 2, the numerical solution matches very well the theoretical one. In particular, both the amplitude and the frequency ( $\nu \simeq 0.025$  Hz) show an excellent agreement between theory and simulations. To further illustrate this overall excellent agreement, in Figure 3 we show the residuals between the theoretical solution and the gravitational wave emission of the close white dwarf binary system in circular orbit. Note that the scale in this case is one order of magnitude smaller than that of Figure 2. Hence, we conclude that our SPH simulations can accurately compute the emission of gravitational waves from coalescing white dwarfs.

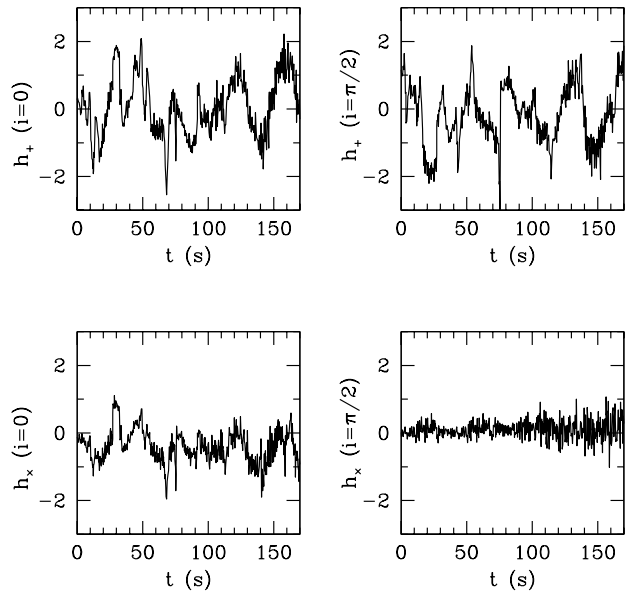


**Figure 3.** Residuals between the theoretical solution and the gravitational wave emission from the close white dwarf binary system of Fig. 2. Note that the dimensionless strains  $h_+$  and  $h_x$  are measured in units of  $10^{-23}$ , one order of magnitude smaller than the scale of Fig. 2.

## 5 GRAVITATIONAL WAVE EMISSION

We have computed the emission of gravitational waves resulting from the merging of several close white dwarf binary systems. In particular, the radiation of gravitational waves from a  $0.4+0.4 M_{\odot}$  He-He, a  $0.4+1.2 M_{\odot}$  He-ONe, a  $0.6+0.8$ , a  $0.6+1.0$  and a  $0.8+1.0 M_{\odot}$  CO-CO was computed. All the simulations performed so far are listed in Table 1, where the mass of both components of the binary system, their respective composition, the initial separation ( $R_0$ ) and the simulation time can be found. For the sake of conciseness we will only discuss in some detail the results of the  $0.4+0.4 M_{\odot}$  He-He system and of the  $0.8+1.0 M_{\odot}$  CO-CO merger. In all the cases the initial separation was larger than the corresponding Roche lobe radius of the less massive component. For instance, for the case in which a  $0.4+0.4 M_{\odot}$  He-He merger is considered the initial separation was  $\simeq 0.042 R_{\odot}$ , and in the case of a  $0.8+1.0 M_{\odot}$  CO-CO system the initial separation was  $\simeq 0.027 R_{\odot}$ . Instead of computing self-consistently the chirping phase we have chosen to add a very small artificial radial acceleration term which decreases the separation of both components until the last stable orbit is reached. This acceleration term is proportional to the velocity, never amounts to more than a 5% of the real orbital acceleration and is added once the stars have already done a full orbit, then we let the system relax during another orbit and the whole procedure is repeated again until the secondary fills its Roche lobe. Once the secondary fills its Roche lobe this acceleration term is suppressed and the system is allowed to evolve freely. Nevertheless, we have checked (see §6) that the amplitude of the gravitational waves during the initial phase of the coalescence agrees with that of the chirping phase. Finally,

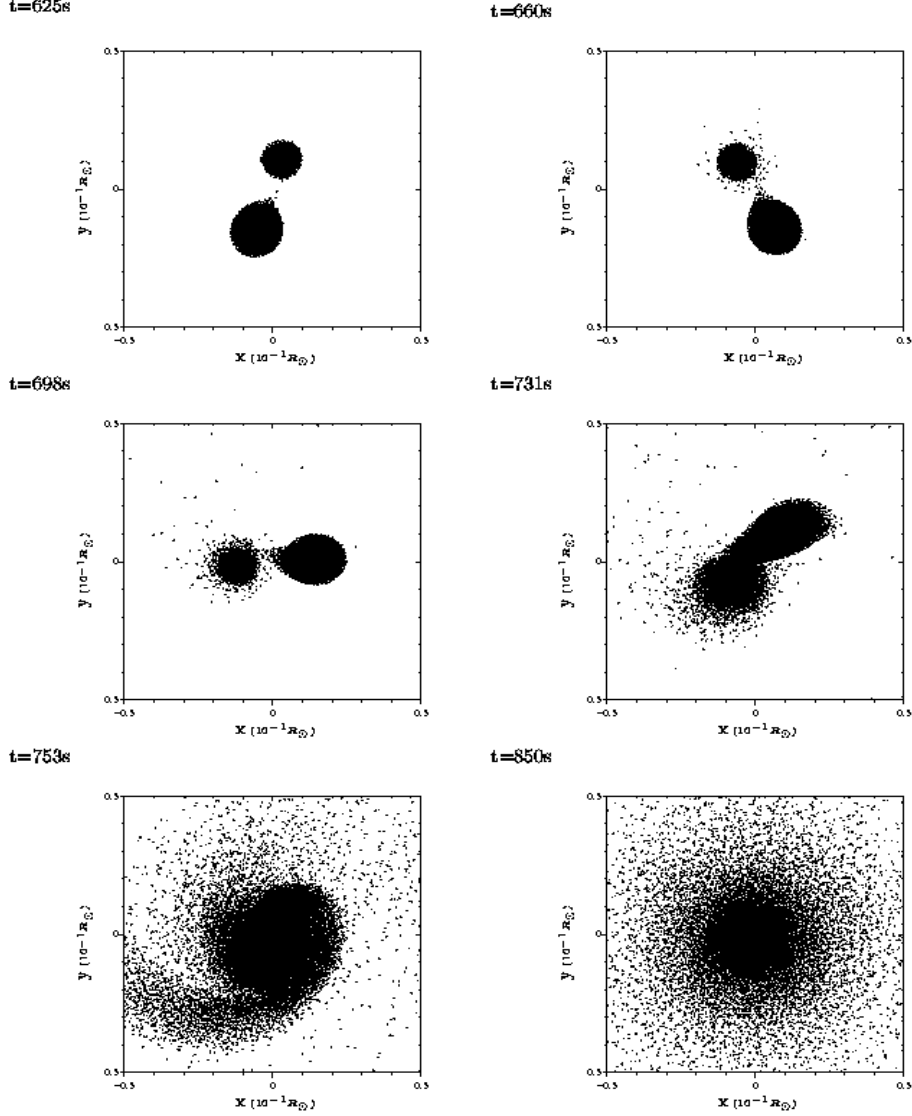


**Figure 4.** Temporal evolution of the  $0.8+1.0 M_{\odot}$  CO-CO close white dwarf binary system during the most important phases of the merger. The SPH particles have been projected in the orbital plane. See text for additional details.

it is important to mention here that in all the simulations studied in the present work the number of particles for each white dwarf is  $2 \times 10^4$  in all cases. However, and in order to check the sensitivity of our results to the number of particles, we have run an additional simulation in which the number of particles was significantly increased to  $2 \times 10^5$  for each star, this simulation is listed in the last entry of table 1 and discussed below.

In Fig. 4 we show the temporal evolution of the positions of the SPH particles projected on to the orbital plane as a function of time for the  $0.8 + 1.0 M_{\odot}$  system. The initial configuration of the two stars was completely spherically symmetric. After some time the secondary is tidally deformed (top left panel) and begins to overflow its Roche lobe (top right panel). As a consequence, an accretion stream forms (middle left panel). This accretion stream is directed

towards the primary, forming an arm. The particles flowing from the secondary onto the primary are redistributed over the surface of the primary (middle right panel) and the arm twists as time increases (bottom left panel), leading to the formation of a heavy accretion disk with cylindrical symmetry (bottom right panel). The whole process lasts for about 3.8 minutes. The merging process can be understood in terms of the positive feedback experienced by the secondary: as the coalescence proceeds the secondary loses mass and, thus, becomes less dense and expands leading to an enhanced mass-loss rate which, in turn, leads to a decrease of the average density of the secondary. Very few particles achieve velocities larger than the escape velocity and, hence, a very small fraction of the total mass is ejected from the system (about  $6.5 \times 10^{-3} M_{\odot}$  in this case). An important feature of the simulation is that the accretion disk

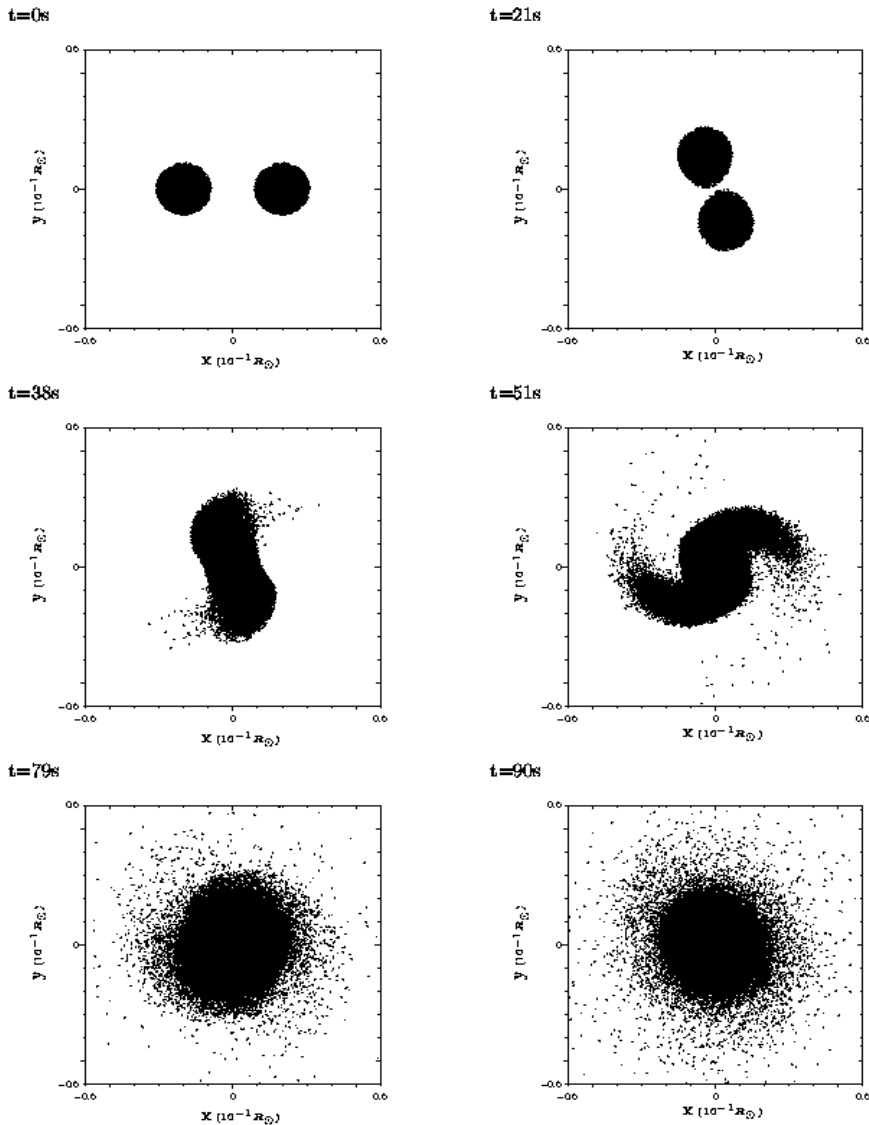


**Figure 5.** Same as figure 4 for the  $0.6+0.6 M_{\odot}$  CO-CO close white dwarf binary system in which  $2 \times 10^5$  SPH particles were used. Only 1 out of 4 particles are shown.

is supported by its own rotational velocity. However, it is important to realize that in the final configuration a weak spiral pattern can still be found. This pattern should become less and less apparent as time increases, reaching cylindrical symmetry during the very late stages of the simulation. However, following the long term evolution of this heavy accretion disk would require a heavy computational load which is well beyond our current possibilities. Additionally, the accretion rate onto the primary becomes negligible during this phase. Hence, our final configuration consists in a central rotating spherically symmetric compact star surrounded by a keplerian and almost cylindrically symmetric accretion disk. As discussed in Guerrero et al. (2004) the rotational velocity of the central star has been probably overestimated due to the large shear introduced by SPH methods. We have used the artificial viscosity of Balsara (1995), which does

not produce an excessive shear and, consequently, reduces somewhat (but not completely) these problems. Therefore, some properties of the merged object could be affected by the excess of rotation of the primary. However, since even in this case the star preserves spherical symmetry we consider that the calculations described below provide a good approximation to the emission of gravitational waves. All the cases studied present more or less the same features except those in which two white dwarfs of equal mass are involved. In such a case the final configuration is a single spheroidal central object — see, for instance, Fig. 5 of Guerrero et al. (2004).

In figure 5 the coalescence of a binary system of  $0.6+0.6 M_{\odot}$  in which each of the stars was modelled using  $2 \times 10^5$  particles is displayed. As in figure 4 we have chosen to represent the temporal evolution of the SPH par-

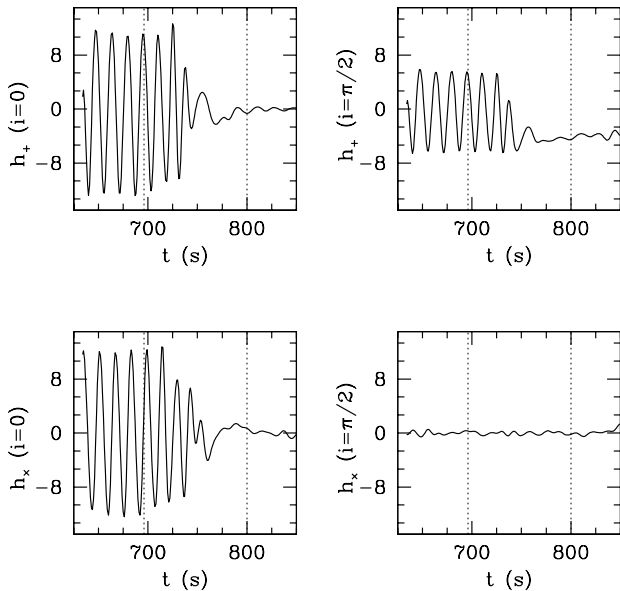


**Figure 6.** Gravitational wave emission from the merger of a  $0.8+1.0 M_{\odot}$  CO-CO close white dwarf binary system. The dimensionless strains  $h_+$  and  $h_{\times}$  are measured in units of  $10^{-22}$ . The leftmost thin dotted line corresponds to the time at which the two white dwarfs start to merge and the rightmost thin dotted line corresponds to the time at which an approximate cylindrical configuration has been already achieved. Again, the source is assumed to be at a distance of 10 kpc.

ticles projected in the orbital plane. Note, however, that in this case only one out of four particles has been represented. In this case, however, the simulation only covers times larger than that at which the last stable orbit of the system occurs. As it can be seen, the results are essentially the same and, thus, we are confident in the main results and general trends of our numerical simulations. We will, however, come back later to this issue at the end of this section, when discussing the emission of gravitational waves.

An example of our results is shown in figures 6 and 7, where the dimensionless strains  $h_+$  and  $h_{\times}$  as a function of time for different inclinations are respectively shown for the  $0.8+1.0 M_{\odot}$  CO-CO and the  $0.4+0.4 M_{\odot}$  He-He systems. The beginning and the final time of the merging itself are shown in both figures as thin dotted lines. In figure 6 it can be seen that before the coalescence proceeds the emission of gravitational waves still has a sinusoidal pattern, but with an increasing frequency. That is, the close white dwarf binary system chirps as a consequence of the spiral trajectory of the stars towards the center of mass. Note that  $h_{\times}$  for  $i = \pi/2$  is zero because the orbital plane is parallel to the line of sight. When the two white dwarfs start to coalesce, the amplitude of the dimensionless strains somehow increase first, but only during the first (and most violent) stage of the merger. This corresponds to the phase in which a spiral arm is formed. After the second maximum is achieved the amplitude decreases dramatically. In fact, only two more clear maxima can be apparently distinguished before the system reaches its final configuration. It is interesting to note that

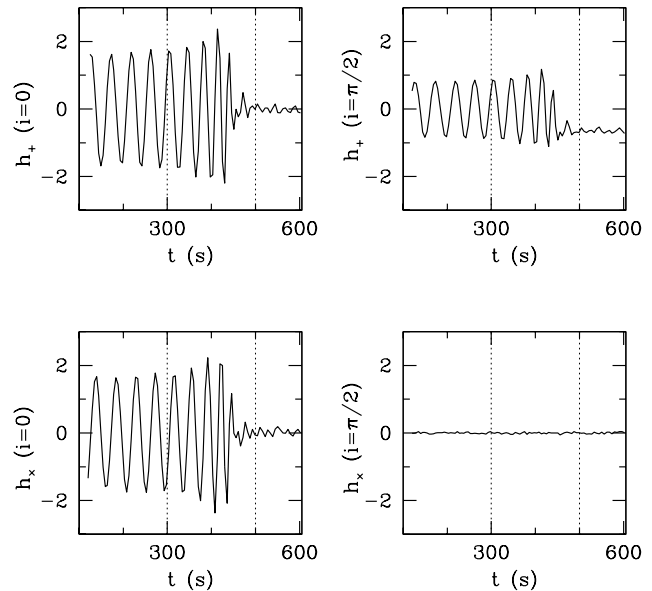


**Figure 7.** Same as Fig. 6 but for the case of a  $0.4+0.4 M_{\odot}$  He-He close white dwarf binary system.

once the merger has already finished one of the dimensionless strains still is significant,  $h_+ \simeq -5 \cdot 10^{-22}$  at  $d = 10$  kpc for  $i = \pi/2$ . This residual emission is due to the inhomogeneities of the accretion disk previously discussed. Each one of the very small maxima appearing at very late times corresponds to successive crossings of the edge of the weak spiral arm in front of the line of sight. Note as well that this residual emission tends to disappear asymptotically, as a consequence of the ongoing rehomogenization of the accretion disk. It is important to realize that these inhomogeneities could be either an artifact due to the resolution used in our SPH simulations or a consequence of the adopted artificial viscosity, since it is well known that the artificial viscosity of Balsara (1995) induces a considerable shear viscosity.

In figure 7 it can be seen that although during the first part of simulation the same chirping pattern is found, once the merger proceeds the gravitational wave signal suddenly disappears on a short time scale, comparable to the orbital period. This is due to the fact that in this case the two stars have equal masses and, therefore, there is not a prominent spiral accretion stream. Instead the two components of the binary system are disrupted around the center of masses, where a shocked region forms as a consequence of the impact between two streams. The typical Mach numbers in the shocked region are  $\text{Ma} \sim 1$ . The streams are slightly asymmetric, depending on the orbital phase at which they form. By the end of the simulation — see again Fig. 5 of Guerrero et al. (2004) — both streams become entangled and the final configuration of the resulting object consists in a central shocked region surrounded by a less dense rotating spheroid, in which a certain degree of asymmetry is still present. Hence, the coalescing process does not present a rather symmetric behavior during the initial phases and, consequently, we see three consecutive maxima. After this, once the streams become entangled the emission of grav-

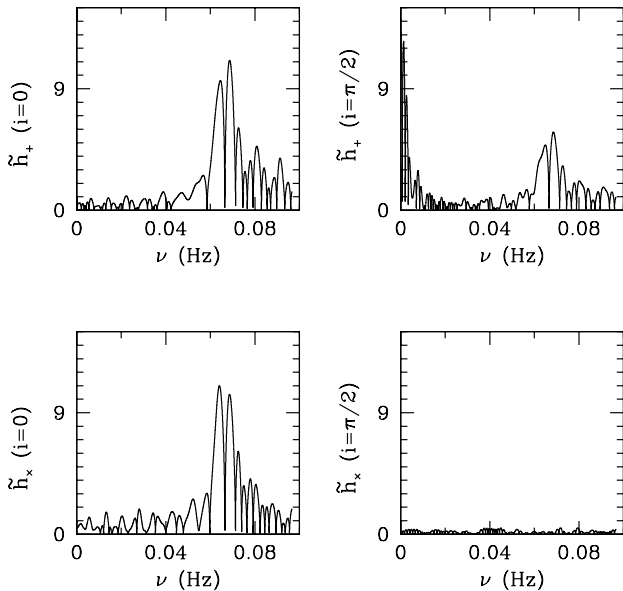


**Figure 8.** Modulus of the Fast Fourier Transform of the adimensional strains  $h_+$  and  $h_x$  of Fig. 6.

itational waves is heavily suppressed and, by the end of the merging process, the emission of gravitational waves is negligible. However, note as well that in this case a small residual emission is also observed in the dimensionless strain  $h_+ = -0.8 \cdot 10^{-22}$  at  $d = 10$  kpc for  $i = \pi/2$ , although considerably smaller than in the previous case. This is again due to our limited computational resources. The impossibility of following the very late phases of the coalescence episode does not allow us to compute the rehomogenization of the external spheroid and, hence, to compute the long-term behavior of  $h_+$  accurately.

The same information is displayed in figures 8 and 9, but in a different format. As can be seen there, the dominant frequency is given by the orbital period. However, as the components of the binary system approach each other, the dominant frequency is shifted to larger values and, during the merger, high frequencies show up, although with very low amplitudes.

Finally, and in order to check the sensitivity of our results to the resolution of the SPH simulations described above we have computed the emission of gravitational waves for both our run “7”, in which  $2 \times 10^5$  particles were used for each star, and our run number 3, in which a resolution 10 times poorer was adopted. The results are displayed in Fig. 10. As in the previous figures the vertical thin lines denote the moment at which the last stable orbit is achieved. Note, nevertheless, that the high resolution simulation was started, as previously mentioned, when the system was already at the last stable orbit. That is the reason why the chirping phase does not appear. Consequently, the time origin of this simulation has been shifted accordingly to match that of the low resolution simulation. As it can be seen the emission of gravitational waves is very similar in both cases, and, hence, our results are robust.

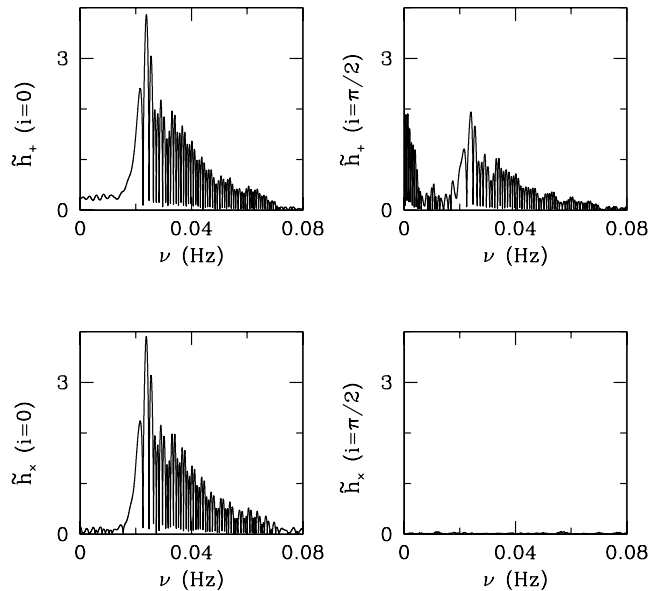


**Figure 9.** Modulus of the Fast Fourier Transform of the adimensional strains  $h_+$  and  $h_x$  of Fig. 7.

## 6 DETECTABILITY

In order to check whether or not LISA would be able to detect a close white dwarf binary system we have proceeded as follows. We have already shown that the most prominent feature of the emitted signal is its sudden disappearance in a couple of orbital periods and that the gravitational wave emission during the coalescence phase does not increase noticeably. Hence, the gravitational wave emission is dominated by the chirping phase. Hence, we have assumed that the orbital separation of the two white dwarfs is exactly that of our binary system *when mass transfer starts*. We have done so because, as explained before, we have added a small artificial acceleration term to the initial configuration in order to avoid an excessive computational demand at the very beginning of our simulations. This acceleration term is suppressed once the secondary begins to transfer mass onto the primary. Note, however, that the mass transfer starts when the secondary fills its Roche lobe and, consequently, this orbital separation is physically sound. We have further assumed that the integration time of LISA will be one year. We have checked that during this period the variation of the orbital separation is negligible (see also figures 6 and 7). Of course, should the integration time be smaller the signal-to-noise ratio derived below would be smaller. Hence, our results should be regarded as an upper limit.

The signal-to-noise ratio,  $\eta$ , is given by

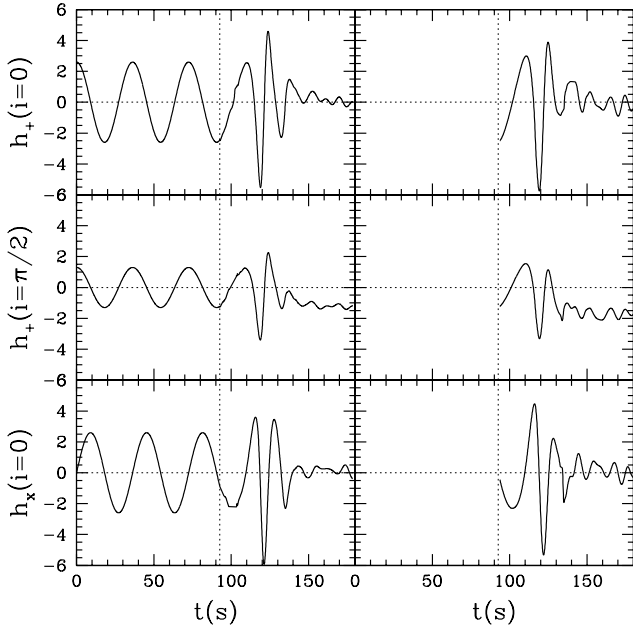
$$\eta^2 = \int_{-\infty}^{+\infty} \frac{\tilde{h}^2(\omega)}{S(\omega)} \frac{d\omega}{2\pi} \quad (14)$$

where  $S(\omega) = S_h(\omega)\tau$  is the sensibility of LISA,  $\tau$  is the integration period, and  $\tilde{h}(\omega)$  is the Fourier Transform of the dimensionless strain. It can be easily shown that for a monochromatic gravitational wave  $\eta = h(\omega)/S_h^{1/2}(\omega)$ . The



**Table 2.** Maximum distance at which LISA will detect the close white dwarf binary systems discussed in this paper, see text for details.

Run	$M_{\text{tot}}$ ( $M_{\odot}$ )	$\nu_0$ (mHz)	$M$ ( $M_{\odot}$ )	$d_{\text{max}}$ (kpc)	$\eta$ (10 kpc)	$h_{\text{max}}$ ( $10^{-22}$ )	$E$ ( $10^{41}$ erg)
1	0.4+1.2	32	0.59	21	10.5	11.4	6
2	0.4+0.4	21	0.35	10	5.0	2.4	0.1
3	0.6+0.6	13	0.53	26	13.0	6.0	0.6
4	0.6+1.0	34	0.67	29	14.5	6.8	2
5	0.6+0.8	40	0.60	31	15.6	6.1	1
6	0.8+1.0	58	0.77	33	16.6	12.8	7
7	0.6+0.6	13	0.53	26	12.8	5.9	0.6


**Figure 10.** A comparison of the computed emission of gravitational waves when the resolution of our SPH simulations is changed. The left panels show the emission of gravitational waves for a simulation in which a low resolution ( $2 \times 10^4$  SPH particles) was used. The right panels show the same quantities when a high resolution was adopted ( $2 \times 10^5$  SPH particles). See text for further details.

maximum distance,  $d_{\text{max}}$ , at which LISA would be able to detect a close white dwarf binary system is then:

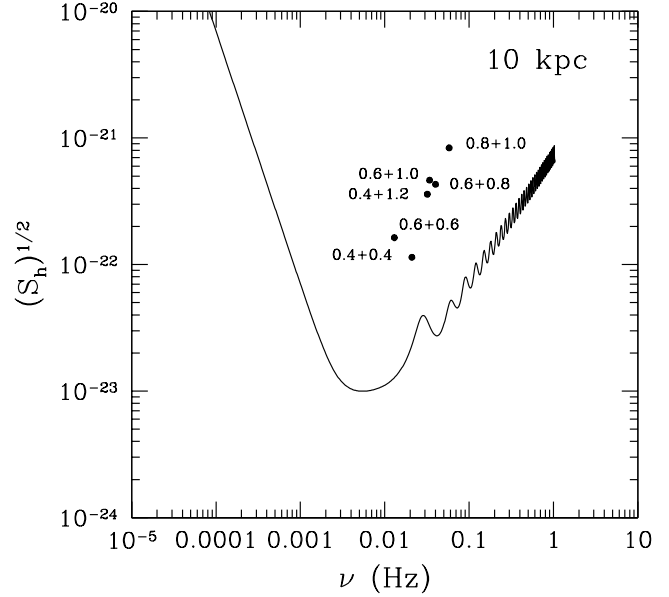
$$d_{\text{max}} \approx 17 \left( \frac{5}{\eta} \right) \left( \frac{M}{M_{\odot}} \right)^{5/3} \left( \frac{\nu_0}{1 \text{ mHz}} \right)^{2/3} \left( \frac{10^{-23}}{\sqrt{S_h(\nu_0)}} \right) \text{ kpc} \quad (15)$$

where  $\nu_0$  is the frequency of gravitational wave, and  $M$  is the chirping mass.

$$M = (\mu M_{\text{tot}}^{2/3})^{3/5} \quad (16)$$

being  $\mu = m_1 m_2 / M_{\text{tot}}$  the reduced mass, and  $M_{\text{tot}} = m_1 + m_2$  the total mass.

In order to evaluate the maximum distance at which LISA would be able to detect the close white dwarf binary systems studied here we have adopted  $\eta = 5$ . We have furthermore used the integrated sensibility of LISA as obtained from <http://www.srl.caltech.edu/~shane/sensitivity>.


**Figure 11.** A comparison of the signal produced by the close white dwarf binary systems studied here, when a distance of 10 kpc is adopted, with the spectral distribution of noise of LISA for a one year integration period.

The results are given in Table 2, where the frequency of the close white dwarf binary system when the secondary overflows its Roche lobe, the chirping mass, the maximum distance at which LISA would detect them for a signal-to-noise ratio of 5 and one year integration, and the signal-to-noise ratio at 10 kpc for one year integration are shown. Also shown in Table 2 are the peak amplitude at 10 kpc of the dimensionless strain (in units of  $10^{-22}$ ) and the total radiated energy in the form of gravitational waves. We stress that if the merger occurs during the one year integration period the signal-to-noise ratio would be smaller. It is worth noticing as well that the energy radiated away from the binary system during the coalescence in the form of gravitational waves is of the order of  $\sim 10^{41}$  erg, much smaller than the total energy of the system and, hence, totally negligible in the energy budget, so no back reaction should be taken into account and the procedure used here is robust. Note as well, that for the case of  $0.6 + 0.6 M_{\odot}$  system, in which two resolutions were used the maximum distance at which LISA

would be able to detect the coalescence is very similar for both the high resolution simulation, 12.8 pc, and the low resolution simulation, 13.0 pc. The energy released during the coalescence is very similar as well in both cases, 0.63 and  $0.64 \times 10^{41}$  erg, respectively.

Finally, in Fig. 11 we compare the signal produced by the close white dwarf binary systems studied in this paper, when a distance of 10 kpc is adopted, with the spectral distribution of noise of LISA for a one year integration period. As it can be seen, all of them will be eventually detected, at different signal-to-noise ratios, ranging from  $\sim 5.0$  for the  $0.4 + 0.4 M_{\odot}$  system to  $\sim 16.6$  for the  $0.8 + 1.0 M_{\odot}$  system.

## 7 DISCUSSION AND CONCLUSIONS

We have computed the emission of gravitational waves of merging white dwarf binaries, for a wide range of masses and compositions of the components of the binary system. For that purpose we have used a SPH code which allowed us to follow the temporal evolution of the coalescing white dwarfs. We have shown that the most noticeable feature of the emitted signal is a sudden disappearance of the gravitational strains. By contrast the chirping phase will be easily detectable by future space-borne interferometers like LISA. In fact, it can be said that the most relevant signature of the merger will be the absence of any signature and the sudden disappearance of the source. Since the frequency coverage of LISA will range from  $10^{-1}$  to  $10^{-4}$  Hz, the detection of chirping close white dwarf binary systems is guaranteed (Farmer & Phinney 2003; Nelemans et al. 2001a). Moreover, at frequencies of  $\sim 3 \cdot 10^{-3}$  Hz most close white dwarf binary systems will be spectrally resolved (Cornish & Larson 2003). Typically, LISA will be able to detect  $\sim 3000$  binaries at these frequencies (Seto 2002). Additionally, it has been recently shown (Cooray, Farmer & Seto 2004) that the typical error box of LISA for these kind of systems will be  $\delta\Omega \sim 5 \text{ deg}^2$ , and that, given that many of the detected sources will be eclipsing binaries with a period equal to that of the gravitational waves, optical follow-up campaigns will allow us to further constrain the location of the sources. Hence, by combining optical observations and gravitational wave data, and taking into account that the gravitational wave signal for such mergers suddenly vanishes — or, equivalently, that during the integration period the signal-to-noise ratio stops growing — we should be able to gain insight into the physics of merging and to obtain precise information of the properties of the progenitor systems. Moreover, it should be taken into account that for a typical merger — namely, the  $0.6 + 0.8 M_{\odot}$  case — the volume accessible to LISA is  $V_{\text{LISA}} \sim 1.2 \times 10^{14} \text{ pc}^3$ . Since the volume of the Galaxy is  $V \sim 3 \times 10^{11} \text{ pc}^3$ , LISA would be able to detect all the mergers occurring in our Galaxy during its operation period. However, the typical rate of white dwarf mergers is  $r \sim 8.3 \times 10^{-3} \text{ yr}^{-1}$  (Nelemans 2003) and, hence, although there is an uncertainty of a factor of 5 in the rate of white dwarf mergers, the expected detection rate is consequently small.

and by the CIRIT. We would also like to acknowledge the invaluable advice of J.M. Ibáñez who largely contributed through his support, suggestions and comments to improve the manuscript. We also thank our anonymous referee for valuable comments and criticisms.

## REFERENCES

- Abramovici, A., et al., 1992, *Science*, **256**, 325
- Acernese, F., et al., 2004, *Class. & Quantum Grav.*, **21**, S385
- Balsara, D., 1995, *J. Comp. Phys.*, **121**, 357
- Barnes, J., & Hut, P., 1986, *Nature*, **324**, 446
- Bender, P.L., et al., 1998, “*LISA: Laser Interferometer Space Antenna for the detection and observation of GW*”, Pre-fase A Report (Garching: Max Planck-Institut für Quantenoptik)
- Bender, P.L., et al., 2000, “*LISA: a cornerstone mission for the observation of gravitational waves*”, ESA-SCI(2000)11, System and Technology Study Report
- Benz, W., 1990, in “*The numerical modelling of Nonlinear stellar Pulsations*”, Ed.: J. Buchler, (Dordrecht: Kluwer Academic Publishers), 269
- Benz, W., Hills, J.G., Thielemann, F.-K., 1989, *ApJ*, **342**, 986
- Cooray, A., Farmer, A.J., & Seto, N., 2004, *ApJ*, **601**, 47L
- Cornish, N.J., Larson, S.L., 2003, *Phys. Rev. D.*, **10**, 103001
- Evans, C.R., Iben, I., & Smarr, L., 1987, *ApJ*, **323**, 129
- Farmer, A.J., & Phinney, E.S., 2003, *MNRAS*, **346**, 119
- Gingold, R.A., & Monaghan, J.J., 1977, *MNRAS*, **181**, 375
- Guerrero, J., García-Berro, E., & Isern, J., 2004, *A&A*, **413**, 257
- Hils, D., Bender, P.L., & Webbink, R.F., 1990, *ApJ*, **369**, 75
- Lucy, L.B., 1977, *AJ*, **82**, 1013
- Mironowski, V.M., 1996, *Soviet Astr.*, **9**, 752
- Misner, C.W., Thorne, K.S., & Wheeler, J.A., 1973, “*Gravitation*” (New York: W.H. Freeman)
- Monaghan, J.J., 1992, *Ann. Rev. Astron. Astrophys.*, **30**, 543
- Monaghan, J.J., & Lattanzio, J.C., 1985, *A&A*, **149**, 135
- Nakamura, T., & Oohara, K., 1989, in “*Frontiers in Numerical Relativity*”, Eds: C.R. Evans, L.S. Finn, & D.W. Hobill (Cambridge: Cambridge Univ. Press) 254
- Nelemans, G., Yungelson, L.R., Portegies Zwart, S.F., & Verbunt, F., 2001a, *A&A*, **365**, 491
- Nelemans, G., Portegies Zwart, S.F., Verbunt, F., & Yungelson, L.R., 2001b, *A&A*, **368**, 939
- Nelemans, G., 2003, in “*The Astrophysics of Gravitational Wave Sources*”, AIP Conf. Proc., **686**, 263
- Rauscher, T., & Thielemann, F.-K., 2000, *Atom. Data & Nucl. Data Tables*, **75**, 1
- Rosswog, S., Davies, M.B., Thielemann, F.-K., & Piran, T., 2000, *A&A*, **360**, 171
- Rosswog, S., & Davies, M.B., 2002, *MNRAS*, **334**, 481
- Rosswog, S., Liebendörfer, M., 2003, *MNRAS*, **342**, 673
- Serna, A., Alimi, J.M., & Chièze, J.P., 1996, *ApJ*, **461**, 884
- Seto, N., 2002, *MNRAS*, **333**, 469
- Schutz, B.F., 1999, *Class. & Quantum Grav.*, **16**, A131
- Takahashi, R., et al., 2004, *Class. & Quantum Grav.*, **21**, S403
- Willke, B., et al., 2004, *Class. & Quantum Grav.*, **21**, S417
- Yungelson, L.R., Livio, M., Tutukov, A.V., & Saffer, R.A., 1994, *ApJ*, **420**, 336